Comparison of the Rheological Properties of Metallocene-Catalyzed and Conventional High-Density Polyethylenes

J. F. Vega, A. Muñoz-Escalona,† A. Santamaría,* M. E. Muñoz, and P. Lafuente†

Departamento de Ciencia y Tecnología de Polímeros, Facultad de Química, Universidad del País Vasco, Apartado 1072, E-20080 San Sebastián, Basque Country, Spain

Received April 4, 1995; Revised Manuscript Received September 22, 1995[⊗]

ABSTRACT: Dynamic measurements in a plate−plate system and steady state flow experiments in a capillary die are presented for conventional high-density polyethylenes (HDPEs) and a new type of polyolefin. The latter, the so-called metallocene-catalyzed HDPEs, are characterized by their low polydispersity and the total absence of branching. The metallocene-catalyzed materials show a different rheological behavior than commercial polyethylenes, which can be summarized as follows: (a) Higher viscosities than conventional HDPEs of the same molecular weight. The dependence of the viscosity on the molecular weight follows a power law equation with an exponent of 4.2 for metallocene catalyzed and 3.6 for conventionals. (b) For high molecular weight materials, the storage modulus overcomes the loss modulus ($G' > G''$) at 190 °C in all frequency ranges. However, for conventional HDPEs, $G'' > G'$ at the same temperature and frequency range. (c) At long relaxation times, the values of $H(\tau)$ spectra of metallocene-catalyzed samples are significantly higher than those which correspond to a conventional sample of practically the same molecular weight. (d) Metallocene-catalyzed HDPEs are difficult to process, as sharkskin and slip-stick effects take place at very low shear rates. The onset of sharskin takes place at $\sigma_{c1} = 0.18$ MPa, and the slip-stick regime occurs at $\sigma_{c2} = 0.25$ MPa, independently of temperature. The values of the plateau modulus, $G_N° = 1.6 \times 10^6$ Pa, and the corresponding molecular weight between entanglements, $M_e = 1830$, found for the metallocene-catalyzed materials, are very similar to those found for conventional polyethylenes. However, the activation energies of flow of the new polymers (7−9 kcal/mol) are slightly higher than those of conventional HDPEs.

Introduction

There is no doubt polyethylene is one of the plastic materials with more utilities in the industry. The properties and processability of this material have evolved together with the catalyst systems development.

The discovery of highly active catalysts in 1980 has led to the establishment of the single-site metallocene catalysts as a highly stereospecific system that can polymerize not only α-olefins but also styrene, cycloolefins, and functional monomers.[1] These catalysts yield polyolefins of very diverse molecular weight distributions (MWD), such as very narrow (polydispersity close to 2) as well as bimodal and trimodal distributions. Very homogeneous materials which allow the incursion of a great variety of cyclic, aliphatic, and aromatic comonomers can be obtained, and also the presence of sort chain branching (SCB) and long chain branching (LCB) can be controlled.[2,3]

This enormous versatility in the molecular design of new polyolefins opens new ways in the field of rheology and processing, in order to try to obtain materials with good physical properties (narrow molecular weight distribution) and processability (bimodal distributions or control of branching). However, few papers have been published on the rheology of these new polymeric materials. Dynamic viscoelastic measurements of polypropylenes obtained via *ansa*-metallocene catalyst systems have been performed by Chien et al.,[4] and steady state viscosity data of α-olefin copolymers made using a single-site catalyst system are reported by Story et al.[5] More recently, Kim et al.[6] compared the melt rheological properties (obtained in an extrusion capillary rheometer) of ethylene/α-olefin copolymers produced via metallocene, vanadium, and Dow's INSITE catalysts, with densities ranging from 0.910 to 0.870 g/cm^3.

In this work we have studied the dynamic viscoelastic and steady state flow properties of a series of metallocene-catalyzed polyethylenes, characterized by their low polydispersity and the total absence of short and long chain branching, in comparison with conventional high-density polyethylenes which contain a certain degree of short chain branching to control the density of the final products.

Experimental Section

Materials and Characterization. A rheological study for three different types of polyolefins based on ethylene has been carried out. We can make a distinction between these materials on the basis of the form and width of their molecular weight distribution, as well as on SCB.

Two of the series are commercial polydisperse high-density polyethylenes (mono- and bimodal). The other one is a new type of polyethylene prepared via a single-site metallocene catalyst system by following the method of Kaminsky et al.[7] using Cp_2ZrCl_2 as catalyst. These new polyethylenes have a narrow polydispersity (close to 2) and neither short (SCB) nor long chain branching (LCB) in their structure. The molecular weight distribution of all samples was measured by GPC, and the level of branching by ^{13}C NMR.

The structural parameters of HDPE grades are listed in Table 1.

The commercial polyethylenes were supplied as pellets and the metallocenes catalyzed as a powder. The latter were stabilized by addition of 0.2 weight % of Irganox 1001 antioxidant.

Rheological Measurements. The viscoelastic functions, storage modulus, $G'(\omega)$, and loss modulus, $G''(\omega)$, of all samples were determined in a Carri-Med CSL-100 rheometer in the dynamic mode with the parallel plates geometry at different

† Repsol Investigación y Desarrollo, Embajadores 183, 28045 Madrid, Spain

⊗ Abstract published in *Advance ACS Abstracts,* January 1, 1996.

0024-9297/96/2229-0960$12.00/0

Table 1. Structural Parameters of HDPE Grades

materials	M_ω	M_ω/M_n	mol % of comonomer and type	branching[a]	total CH_3/1000 C[b]
PE-5502-A[c]	195 500	10.1	0.09/1-hexene	1.08	1.52
PE-6006-L	171 500	7.7	0.15/1-hexene	1.40	2.17
TUB-125[d]	273 000	15.7	0.59/1-butene	3.12	6.08
NCPE-2494	314 000	16.7	0.66/1-butene	3.75	7.01
GM-5010-T2E	318 000	21.8	0.54/1-butene	3.62	6.32
PE01[e]	14 000	2.3		0.00	6.65
PE02	69 000	3.5		0.00	1.44
PE03	194 000	2.9		0.00	0.39
PE04	238 000	3.5		0.00	<0.4
PE05	250 000	2.9		0.00	<0.4

[a] Branches given as CH_3/1000 C atoms. [b] Total CH_3/1000 C including polymer chain-ends and branching. [c] Commercial polydisperse monomodal HDPE (Repsol, Spain). [d] Commercial polydisperse bimodal HDPEs (from Solvay, Neste, and Hoechst, respectively). [e] Metallocene-catalyzed HDPEs (Repsol, Spain) (without any comonomer).

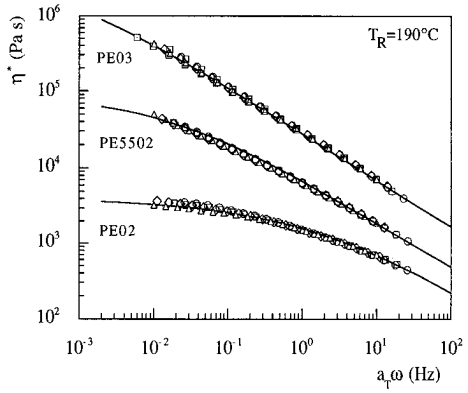

Figure 1. Time−temperature superposition of complex viscosity $\eta^*(\omega)$ for PE03, PE5502A, and PE02 at T_R = 190 °C: (○) 140−145 °C; (□) 160 °C; (◇) 175−180 °C; (△) 190 °C; (⊡) 210 °C. Lines are drawn to guide the eye.

temperatures from 140 to 210 °C. The frequency range was from 10^{-2} to 10 Hz, with an amplitude of 6×10^{-4} rad, which belongs to the lineal viscoelastic region, located with the aid of a previous torque sweep.

These measurements were realized with test specimens (20 mm diameter and 2 mm thickness) molded in a CS-183 Mini-Max molder at 180 °C and 60 rpm for 5 min.

The steady state measurements have been carried out in a Sieglaff McKelvey capillary rheometer in the temperature range 140−220 °C, using a capillary ratio $L/D = 25$. In this case the shear stress and the activation energy of flow were determined by working in the constant velocity mode in a shear rate range from 1 to 100 s^{-1}.

Results and Discussion

Complex Viscosity. The complex viscosity functions, defined as $\eta^* = ((G'/\omega)^2 + (G''/\omega)^2)^{1/2}$, of three of the samples listed in Table 1 are shown in Figure 1, referred to 190 °C.

We remark on the much higher viscosity of the metallocene-catalyzed sample (PE03) compared to the conventional polyethylene (PE-5502-A) of practically the same weight average molecular weight. In the frequency range covered when data are shifted to 190 °C, it is not possible to obtain frequency independent viscosities, except in the case of low molecular weight samples (PE01 and PE02), for which the Newtonian viscosity, η_0, can be inferred. Due to the impossibility of dealing with Newtonian (linear) viscosities, we have correlated the complex viscosity taken at $\omega = 0.01$ Hz, $\eta^*(0.01)$ (which values are listed in Table 2), to molecular parameters like molecular weight and polydispersity.

In Figure 2 we show $\eta^*(0.01)$ data of the polyethylenes of Table 1, together with data taken from the literature,[8−10] as a function of weight average molecular weight. The data can be reasonably adjusted to two straight lines, which makes evident the difference between the metallocene-catalyzed and conventional polyethylenes. This latter group involves commercial polyethylenes (including samples of bimodal molecular weight distribution) and monodisperse fractions (reported $M_\omega/M_n = 1.2$),[8] whose results are well described by the equation proposed by Raju and co-workers[8] for polyethylene fractions at 190 °C:

$$\eta_0 = 3.4 \times 10^{-15}(\bar{M}_\omega)^{3.6} \quad (1a)$$

The data of $\eta^*(0.01)$ for commercial polyethylenes in Figure 2 fit to a straight line:

$$\eta^*(0.01) = 3.2 \times 10^{-15}(\bar{M}_\omega)^{3.6} \quad (1b)$$

where $\eta^*(\omega = 0.01)$ has been used instead of η_0.

On the other hand the results of the metallocene-catalyzed polyethylenes are well fitted to the equation

$$\eta^*(0.01) = 2.3 \times 10^{-17}(\bar{M}_\omega)^{4.2} \quad (2)$$

These results allow us to state that the metallocene-catalyzed polyethylenes, which are characterized by the total absence of short branches, give rise to considerably higher viscosities than the slightly short branched (see Table 1) conventional polyethylenes.

Storage and Loss Moduli. Data of storage $G'(\omega)$ and loss $G''(\omega)$ moduli of three of the samples (the rest have been omitted to avoid crowding) are shown in Figure 3, referred to 190 °C.

The results of two of the samples, PE03 and PE-5502-A, with very similar weight average molecular weights but different polydispersities and degrees of short chain branching (see Table 1), differ substantially. Considerably higher values of both $G'(\omega)$ and $G''(\omega)$ are found for PE03. This sample, in contrast with the low molecular weight metallocene-catalyzed PE02, has what we can define as an elastic-like behavior: the storage modulus overcomes the loss modulus in the whole frequency range.

From plots as those displayed in Figure 3 the dynamic cross-point defined as

$$G_x(\omega_x) = G'(\omega) = G''(\omega) \quad (3)$$

can be determined. Cross-point values, which in fact separate viscous-like and elastic-like behaviors, are included in Table 2. These values, as well as G_x values taken from the literature, are plotted as a function of polydispersity in Figure 4, where we observe that G_x

Table 2. Rheological Parameters of the Materials (T = 190 °C)[a]

material	$\eta^*(0.01)$ (Pa·s)	G_x (Pa)	E_a (kcal/mol)	η_0 (Pa·s)	τ_0 (s)	n
PE-5502-A	5.01×10^4	2.98×10^4	7 (7)	1.43×10^5	87.7	0.55
PE-6006-L	2.20×10^4	3.20×10^4	6.5 (7)	5.40×10^4	32.2	0.62
TUB-125	5.65×10^4	4.93×10^4	5.2 (5.2)	1.09×10^5	13.4	0.55
NCPE-2494	6.50×10^4	3.24×10^4	5.3 (5.4)	1.95×10^5	53.5	0.56
GM-5010	1.02×10^5	1.44×10^4	5.4 (5.3)	4.81×10^5	200	0.47
PE01	4.6					
PE02	3.30×10^3	5.60×10^4	8.1 (8.6)	3.77×10^3	0.347	0.75
PE03	4.30×10^5		8.9	3.5×10^6	976	
PE04	1.3×10^6		7.5 (7)			0.36; $\dot{\gamma} < 10\ s^{-1}$
			(0); $\dot{\gamma} < 10\ s^{-1}$			(0); $\dot{\gamma} < 10\ s^{-1}$
PE05	1.5×10^6		7.1			
Raju et al.[5]	2.6×10^5	2.60×10^5	6.5	3.07×10^5		

[a] The values in parentheses are the measures of E_a in steady state flow experiments.

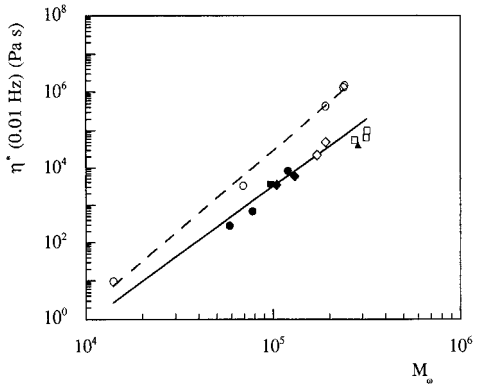

Figure 2. Weight average molecular weight dependence of complex viscosity at ω = 0.01 Hz and T = 190 °C: (○) metallocene catalyzed; (◇) monomodal; (□) bimodal; (●) data of Raju and co-workers;[8] (■) data of Shroff and Shida;[9] (◆) data of Dumoulin and co-workers.[10] The solid line corresponds to eq 1b, and dashed line, to eq 2.

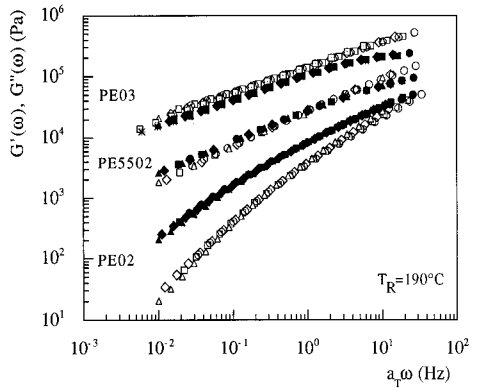

Figure 3. Time−temperature superposition of storage (G') and loss (G'') moduli for PE03, PE5502, and PE02 at T_R = 190 °C: (○,●) 140−145 °C; (□) 160 °C; (◇, ◆) 175−180 °C; (△, ▲) 190 °C; (⊡, *) 210 °C; open symbols, G'; close symbols, G''.

decreases as polydispersity increases. The following equation, proposed by Utracki and Schlund[11] for a series of linear low-density polyethylenes, represents well the tendency of our experimental results:

$$G_x = 8.4 \times 10^5 (\bar{M}_\omega / M_n)^{-1.385} \qquad (4)$$

The plateau modulus, $G_N°$, associated with the entanglement network is the most characteristic viscoelastic parameter at intermediate frequencies and can be estimated from loss modulus data:[12]

$$G_N° = \frac{2}{\pi}\int_{-\infty}^{\infty} G''(\omega)\, d \ln \omega \qquad (5)$$

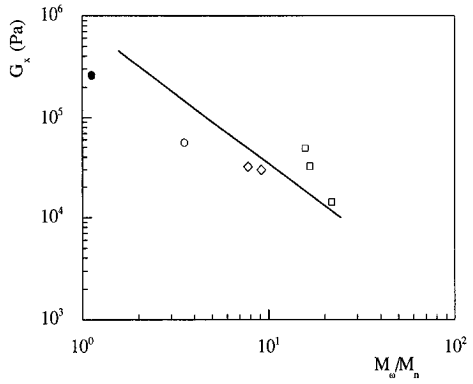

Figure 4. Cross-point modulus, G_x, vs polydispersity, M_ω/M_n, for commercial and metallocene-catalyzed materials: (○) metallocene catalyzed (PE02); (◇) monomodal; (□) bimodal; (●) data of Raju and co-workers;[8] solid line, corresponds to eq 4.

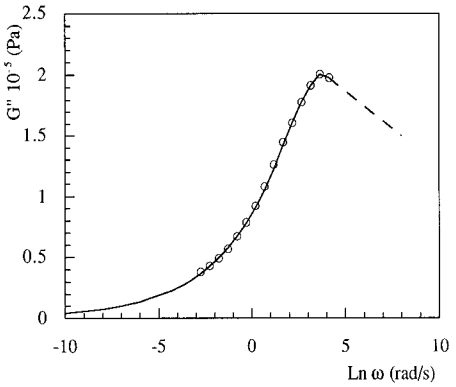

Figure 5. Loss modulus for PE05 at 190 °C, used to determine the plateau modulus $G_N°$.

Only in the case of the metallocene-catalyzed PE05 can eq 5 be used, because data of the other polyethylenes do not extend beyond the maximum in $G''(\omega)$. The value determined at 190 °C from Figure 5 is $G_N° = 1.6 \times 10^6$ Pa, which agrees with the value obtained by Raju et al.[8] for polyethylene fractions. The average molecular weight between entanglements, M_e, is evaluated using the equation based on the theory of rubber elasticity:

$$M_e = \rho RT / G_N° \qquad (6)$$

where ρ is the density, R the gas constant, and T the temperature. Taking a density of ρ = 760 kg/m^3 at T = 463 K, we obtain M_e = 1830.

Notwithstanding our value must be regarded as tentative (we have been able to evaluate $G_N°$ of only one of the samples), we remark that this value coincides with the values of M_e reported for linear (HDPE) and linear low-density (LLDPE) polyethylenes.[13−15] This is

not surprising if we take into account that it has been proved that M_e is not related to large scale parameters but to short-distance chain parameters such as the Kuhn step length, average molecular weight per main chain bond and molecular chain diameter.[16−18] On the other hand if we use the well-established relation between M_e and M_c[19] (the critical molecular weight for the effect of entanglement coupling on viscosity), $M_c = 2M_e$, we obtain a value of $M_c = 3660$. This agrees with the value of the molecular weight at the intersection of the two straight lines of Figure 2; actually combining eqs 1b and 2 yields a value of $M_c = 3735$. We contemplate that the viscosities of both series of metallocene-catalyzed and conventional HDPEs are the same below M_c (following the well-known $\eta_0 \propto M_\omega$ relation) and start to diverge above this characteristic molecular weight. As M_c is the same for both types of HDPEs, we can speculate that the total absence of branches in the metallocene-catalyzed polyethylenes does not give rise to any peculiar behavior (comparing to the slightly branched HDPEs) when chains are unentangled and the viscosity is governed by the monomeric friction factor.[19] However, above the critical molecular weight the large scale structure and the chain configuration are different in both types of polymers, thereby giving rise to a more entangled system (experimentally observed higher viscosity) for metallocene-catalyzed HDPEs.

The temperature dependence of the shift factor a_T used in plotting Figures 1 and 3 can be expressed by the Arrhenius equation:

$$a_T = A \exp(E_a/RT) \tag{7}$$

where A is a constant, which depends on the reference temperature, and E_a is the flow activation energy. In Table 2 we show the values obtained by both dynamic and steady state measurements. For commercial monomodal HDPEs and fractions of narrow polydispersity ($M_\omega/M_n = 1.2$),[8] the values are in the range 6−7 kca/mol, which agrees with literature data.[20−22] However, lower E_a values (5−5.5 kcal/mol) are found for commercial bimodal HDPEs, probably due to the effect of low molecular weight tails. In the case of metallocene-catalyzed polyethylenes, the values of the activation energy of flow are slightly higher and vary in a wider range (7−9 kcal/mol): this variation is not correlated to molecular weight. Actually, our values coincide with those reported by Kim et al.[6] for ethylene/octene copolymers (with long chain branching) obtained by INSITE catalyst (7.8−9.5 kca/mol). At present we do not have an explanation for the fact that pure metallocene, not branched, HDPE homopolymers give rise to higher activation energies of flow than conventional HDPEs.

Relaxation Spectra. The relaxation spectrum of a material at a given temperature points out the concentration of relaxation mechanisms in a specified interval of relaxation times. This spectrum shows clearly the different characteristic zones of viscoelastic behavior, that is, the changes in the melt structure of the polymer in the logarithmic time scale.

There are different ways to determine an approximate relaxation spectrum: from viscoelastic functions (G', G'', J', and J'') using the methods of Ferry−Williams, Tschoelg, Nimomiya−Ferry, and Fujita;[12] from the Carreau model relation for viscosity $\eta'(\omega)$ applied to the first aproximation of Tschoegl;[23] from complex modulus $G^*(\omega)$ using the method developed by Lanfray and Marin;[24] or from the Cole−Cole equation for complex viscosity $\eta^*(\omega)$.[25−27] In this study the last one has been applied, where

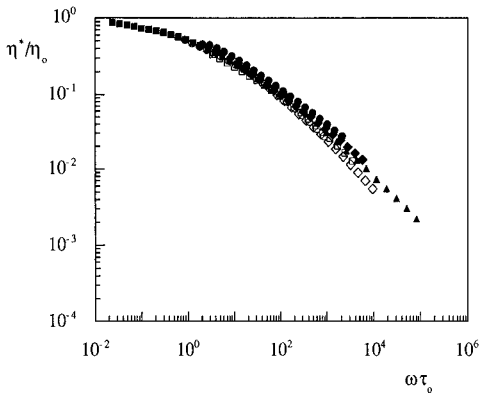

Figure 6. Master curve of η^*/η_0 vs $\omega\tau_0$ for the materials: (◆) PE-5502-A; (●) PE-6006-L; (○) TUB-125; (□) NCPE-2594; (◇) GM-5010-T2E; (■) PE02; (▲) PE03.

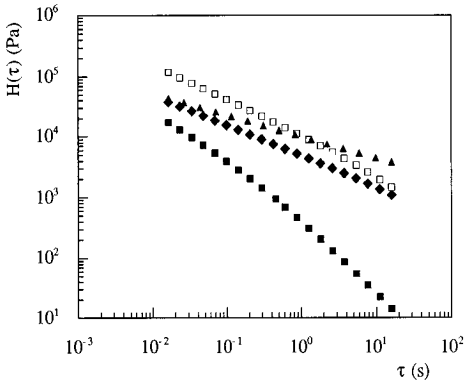

Figure 7. Relaxation spectra at 190 °C calculated by eq 9 for some of the materials. The symbols for each material are the same as in Figure 6.

$$\eta^* = \frac{\eta_0}{(1 + j\omega\tau_0)^{1-\alpha}} \tag{8}$$

η_0 is the zero shear viscosity. α is a characteristic parameter of the distribution relaxation times equal to $2\theta/\pi$ (θ is the angle between the diameter going through the origin and the real axis in the Cole−Cole plot). τ_0 is a time constant, estimated as the inverse of the frequency at which the imaginary part of complex viscosity $\eta''(\omega)$ has a maximum.

In Table 2 we include the values of these parameters which have been determined from Cole−Cole plots of η'' versus η'. Using the values obtained for η_0 and τ_0, we can draw a curve for normalized complex viscosity, η^*/η_0, versus $\omega\tau_0$ (Figure 6). It can be observed that all the experimental data are located on the same master curve. This suggests that τ_0 is related to the longest relaxation time[28,29] at which viscosity decreases due to a diminution in the concentration of entanglements. The values of η^*/η_0 fall below unity from a characteristic frequency, ω, which assigns the onset of non-Newtonian behavior.

This result agrees with the Graessley and William theories[12] for non-Newtonian flow in amorphous/homogeneous polymers.

Using the calculated values of η_0 and τ_0, it is possible to determine the relaxation spectrum in a given range of relaxation times[24] by means of eq 9. We can observe the shape of this function in Figure 7 for various commercial and metallocene-catalyzed polyethylenes.

$$H(\tau) = \frac{2\eta_0(\tau_0/\tau)^{1-\alpha} \sin\theta \cos\theta}{\eta\tau[1 + (\tau_0/\tau)^{2(1-\alpha)} + 2(\tau_0/\tau)^{1-\alpha}(\sin^2\theta - \cos^2\theta)]} \quad (9)$$

The slope of $H(\tau)$ is near $-1/2$, characteristic of the theoretical Rouse relaxation spectrum.[12] The bimodal polyethylenes show higher values than the others, monomodal and metallocene-catalyzed materials, in the interval of relaxation times studied.

The new materials do not show the $-1/2$ slope. On the one hand, in the case of the low molecular weight material (PE02), the slope is greater than this value; it is the typical behavior in the terminal region. On the other hand, an interesting result arises from the comparison between the PE03 and PE-5502-A spectra. These materials have similar molecular weights but different molecular weight distributions and degrees of short chain branching. We can see that the values obtained for the metallocene-catalyzed material are signficantly higher at longer relaxation times, and it can be assumed this is due to a concentration of relaxation mechanisms caused by entanglement couplings between high molecular weight chains in the rubbery or plateau region. In the short time region, close to the transition zone, the spectra are very similar, which suggests that the properties are not affected by the molecular weight distribution.[29,30] In fact, we can observe a common trend of convergence toward this zone of the spectrum for all the materials.

Flow in an Extrusion Capillary Rheometer. The flow curves, obtained by extrusion capillary rheometry, of three of the samples at 160 and 190 °C are shown in Figure 8, and the corresponding viscosity curves are in Figure 9, which includes also complex viscosity η^* data to test the Cox−Merz empirical rule.[31]

We stress once again the higher viscosity of the metallocene-catalyzed sample (PE04) compared to the conventional polyethylene (PE-5502-A), of a similar molecular weight. Moreover the difficulties of processing the metallocene-catalyzed sample are increased as sharkskin surface distortion and slip-stick effects take place at very low shear rates ($\dot{\gamma} = 2$ and $\dot{\gamma} = 10$ s^{-1}, respectively). The sharkskin effect occurs at $\sigma_{c1} = 0.18$ MPa, independently of temperature: this value is slightly lower than the value determined by Utracki and Gendron[32] for a series of HDPE and LLDPE and by Kalika and Denn[33] for an LLDPE. On the other hand a value of $\sigma_{c1} = 0.1$ MPa was determined by Ramamurthy[34] for an LLDPE. The slip-stick regime occurs at a value of $\sigma_{c2} = 0.25$ MPa. In Figure 8 we observe that the lower viscosities of the conventional polyethylene and low molecular weight metallocene-catalyzed polyethylene avoid the appearance of distortions, since shear stresses above σ_c are not attained for these polymers, in the range of shear rates covered. Photographs of sharkskin and slip-stick effects of PE04 are shown in Figure 10.

One of the consequences of the apparition of slip-stick is that the effect of temperature on viscosity vanishes, as the activation energy drops from $E_a = 7$ kcal/mol (Table 2) to $E_a = 0$. This abrupt change has also been reported by other authors.[32] The flow curves of Figure 8 have been adjusted to the well-known power law expression:

$$\sigma_{21} = m\dot{\gamma}^n \quad (10)$$

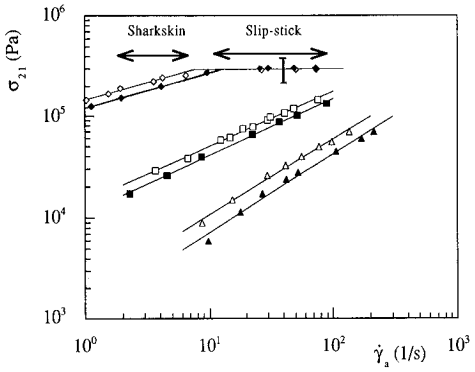

Figure 8. Capillary data for PE04, PE-5502-A, and PE02 at 160 and 190 °C: (◇, ◆) PE04; (□, ■) PE-5502-A; (△, ▲) PE02; open symbols, 160 °C; closed symbols, 190 °C. The vertical bar indicates the amplitude of the oscillations of shear stress values when slip stick takes place. Symbols represent average values.

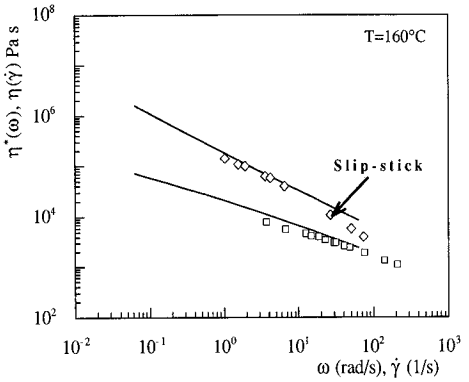

Figure 9. Complex viscosity, η^* (solid lines), and shear viscosity, η (symbols): (◇) PE04; (□) PE-5502-A.

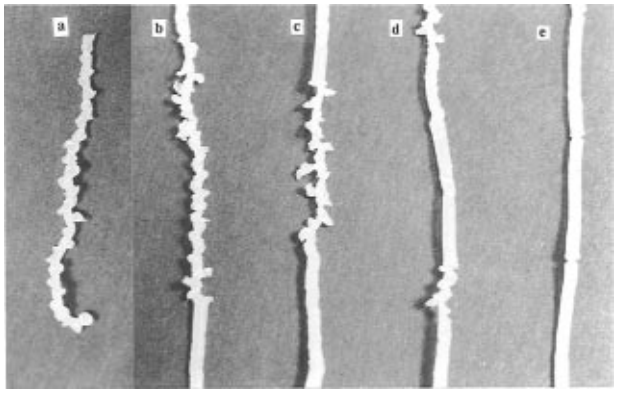

Figure 10. Photographs of sharkskin and slip-stick effects for PEO4: (a) $\dot{\gamma} = 2$ s^{-1}; (b) $\dot{\gamma} = 24.3$ s^{-1}; (c) $\dot{\gamma} = 30.0$ s^{-1}; (d) $\dot{\gamma} = 48.8$ s^{-1}; (e) $\dot{\gamma} = 72.2$ s^{-1}.

and the corresponding values of exponent n are presented in Table 2.

We remark that for polyethylenes of similar molecular weights, the metallocene-catalyzed polymers give rise to lower n values than the conventional ones. On the other hand when the slip-stick effect appears, the exponent n falls to zero, a result already observed for LLDPEs.[33] It is worth pointing out that the measurements taken before and during the occurrence of sharkskin can be adjusted to the same straight line, with an exponent $n = 0.36$ which coincides with the value found by El Kissi and Piau[35] for an LLDPE sample. These authors show that the same power law equation can be used to adjust data of smooth and distorted extrudates, which allow them to demonstrate that the slip velocity

can be zero even when the sharkskin effect takes place. This argument and the hypothesis used by Kalika and Denn,[33] according to which slip accompanies the initiation of surface roughness, are in contradiction. Due to the lack of sample we have not achieved analysis of the slip velocity and therefore we cannot assert whether slip takes place during sharkskin or not. However our results coincide with those of El Kissi and Piau[35] in what concerns the use of the same power law equation for smooth and sharkskin extrudates (see Figure 8). Certainly, the slip-stick effect, which takes place at higher shear rates, is a consequence of the plug-like flow which in turn gives rise to $n = 0$ and $E_a = 0$.

Conclusions

The narrow molecular weight distribution and the total absence of branches determine the rheology of metallocene-catalyzed polyethylenes, compared to conventional HDPEs which have higher polydispersities and a certain degree of SCB. The main rheological features of those new polyethylenes are the following:

(a) The data of η^* (taken at $\omega = 0.01$ Hz and 190 °C) versus M_ω cannot be adjusted by the equation which fits conventional polyethylenes of different modality and polydispersity. In the case of metallocene-catalyzed polyethylenes an exponent of 4.2 is found for the power law equation of $\eta^*(0.01)$ vs M_ω data, instead of the exponent 3.6 found for conventional polyethylenes.

(b) When polyethylenes of almost the same molecular weight are compared, considerably higher values of $G'(\omega)$ and $G''(\omega)$ are found for metallocene-catalyzed than for conventional polyethylenes. However, the plateau modulus, $G_N°$, obtained for only one of the metallocene-catalyzed samples, and the critical molecular weight M_c are similar in both types of polymers.

(c) The values of the spectra of relaxation times of metallocene-catalyzed polyethylenes are significantly higher, at long relaxation times, than those corresponding to conventional polyethylenes of practically the same molecular weight.

(d) The high viscosities of metallocene-catalyzed samples allow them to overcome a critical shear stress ($\sigma_{c1} = 1.8 \times 10^5$ Pa) for the onset of sharkskin, at very low shear rates. This makes difficult the processability of these polyolefins. On the other hand the same power law equation can be used to adjust σ_{21} vs $\dot{\gamma}_{21}$ data of smooth and sharkskin extrudates.

Acknowledgment. We thank Repsol Química for permission to publish this work. Financial support by "Fondos de Cooperación Aquitania-Euskadi-Navarra" is acknowledged. J.F.V. thanks the Government of the Basque Country for a research fellowship.

References and Notes

(1) Sasaki, T.; Ebara, T.; Johiji, H. *Polym. Adv. Tech.* **1993**, *4*, 406−414.
(2) Schwank, D. *Mod. Plast. Int.* **1993**, August, 40−41.
(3) Garbassi, F.; Gila, L.; Proto, A. *Polym. News* **1994**, *19*, 367−371.
(4) Chien, J. C. W.; Linas, G. H.; Rausch, M. D.; Lin, Y. G.; Winter, H. H.; Atwood, J. L.; Bott, S. C. *J. Polym. Sci., Part A: Polym. Chem.* **1992**, *30*, 2601−2617.
(5) Story, B. A.; Knight, G. W. Catalyst Consultants Inc., MetCon '93, Houston, May 26−28, 1993.
(6) Kim, Y. S.; Chung, C. I.; Lay, S. Y.; Hyun, K. S. *ANTEC* **1995**, May, 1122−1129.
(7) Kaminsky, W.; Hahnsen, H.; Külper, K.; Wöldt, R. U.S. Patent 4,542,199, 1985.
(8) Raju, V. R.; Smith, G. G.; Marin, G.; Knox, J. R.; Graessley, W. W. *J. Polym. Sci., Polym. Phys. Ed.* **1979**, *17*, 1183−1195.
(9) Schroff, R. N.; Shida, M. *J. Polym. Sci., Part C: Polym. Symp.* **1971**, *35*, 153−163.
(10) Dumoulin, M. M.; Utracki, L. A.; Lara, J. *J. Polym. Eng. Sci.* **1984**, *24*, 117−126.
(11) Utracki, L. A.; Schlund, B. *Polym. Eng. Sci.* **1987**, *27*, 367−379.
(12) Ferry, J. D. *Viscoelastic Properties of Polymers*, 3rd ed.; John Willey and Sons: New York, 1980.
(13) Schreiber, H. P.; Bagley, E. B. 11th Canadian High Polymer Forum, Windsor, Canada, September 5−7, 1962.
(14) Porter, R. S.; Johnson, J. F. *Chem. Rev.* **1966**, *66*, 1−27.
(15) Carella, J. M.; Graessley, W. W.; Fetters, L. J. *Macromolecules* **1984**, *17*, 2775−2786.
(16) Graessley, W. W.; Edwards, S. F. *Polymer* **1981**, *22*, 1429−1334.
(17) Aharoni, S. M. *Macromolecules* **1986**, *19*, 426−434.
(18) Zang, Y. H.; Carreau, P. J. *J. Appl. Polym. Sci.* **1991**, *42*, 1965−1968.
(19) Graessley, W. W. *Adv. Polym. Sci.* **1974**, *17*, 1−179.
(20) Raju, V. R.; Rachapudy, H.; Graessley, W. W. *J. Polym. Sci., Polym. Eng. Sci.* **1979**, *17*, 1223−1235.
(21) Vinogradov, G. V.; Malkin, A. Y. *Rheology of Polymers*; Mir Publishers: Moscow, 1980.
(22) Van Krevelen, D. W. *Properties of Polymers*, 3rd ed.; Elsevier: New York, 1990.
(23) Utracki, L. A.; Schlund, B. *Polym. Eng. Sci.* **1987**, *27*, 1512−1522.
(24) Lanfray, Y.; Marin, G. *Rheol. Acta* **1990**, *29*, 390−399.
(25) Labaig, J. S.; Monge, P.; Bednarick, J. *Polymer* **1973**, *15*, 384−386.
(26) Marin, G.; Labaig, J. J.; Monge, P. *Polymer* **1975**, *16*, 234−226.
(27) Montfort, J. P.; Marin, G.; Monge, P. *Macromolecules* **1984**, *17*, 1551−1560.
(28) Cassagnau, P.; Montfort, J. P.; Marin, G.; Monge, P. *Rheol. Acta* **1993**, *32*, 156−167.
(29) Onogi, S.; Masuda, T.; Kitagawa, K. *Macromolecules* **1970**, *3*, 109−116.
(30) Onogi, S.; Masuda, T.; Kitagawa, K. *Macromolecules* **1970**, *3*, 126−125.
(31) Cox, W. P.; Merz, E. H. *J. Polym. Sci.* **1958**, *28*, 619−622.
(32) Utracki, L. A.; Gendron, R. *J. Rheol.* **1984**, *28*, 601−623.
(33) Kalika, D. S.; Denn, M. *J. Rheol.* **1987**, *31*, 815−834.
(34) Ramamurthy, A. V. *J. Rheol.* **1986**, *30*, 337−357.
(35) El Kissi, N.; Piau, J. M. *J. Rheol.* **1994**, *38*, 1447−1463.

MA9504633